Analytical Biochemistry xxx (2008) xxx–xxx

Contents lists available at ScienceDirect

Analytical Biochemistry

journal homepage: www.elsevier.com/locate/yabio

A coupled assay measuring *Mycobacterium tuberculosis* antigen 85C enzymatic activity

Julie Boucau [a], Aditya K. Sanki [a], Bradley J. Voss [b], Steven J. Sucheck [a], Donald R. Ronning [a,*]

[a] *Department of Chemistry, 2801 W. Bancroft Street, University of Toledo, Toledo, OH 43606, USA*
[b] *Department of Chemistry, Olivet College, Olivet, MI 49076, USA*

ARTICLE INFO

Article history:
Received 29 August 2008
Available online xxxx

Keywords:
Acyltransfer
Mycolyltransferase
Antigen 85C
β-Glucosidase
Drug screening
Enzyme-coupled assay

ABSTRACT

The prevalence of drug-resistant strains of *Mycobacterium tuberculosis* (*M. tb*) emphasizes the need for new antitubercular drugs. An essential component of the drug discovery process is the development of tools to rapidly screen potential drug libraries against important biological targets. Similarly to well-documented *M. tb* targets, the antigen 85 (Ag85) enzymes are involved in the maintenance of the mycobacterial cell wall. The products synthesized by these mycolyltransferases are the cell wall components most responsible for the reduced permeability of drugs into the bacterial cell, thereby linking Ag85 activity directly with drug resistance. This article presents the development of a high-throughput colorimetric assay suitable for direct monitoring of the enzymatic activity. The assay uses a synthetic substrate containing three chemical moieties: an octanoyl fatty acid, β-D-glucose, and *p*-nitrophenyl. In the context of the assay, Ag85 catalyzes the removal of the fatty acid and releases *p*-nitrophenyl-β-D-glucoside. The glucoside is hydrolyzed by β-glucosidase to release the *p*-nitrophenolate chromophore. With this assay, the K_M and k_{cat} values of Ag85C were determined to be 0.047 ± 0.008 mM and 0.062 s^{-1}, respectively. In addition, the assay exhibits a Z' value of 0.81 ± 0.06, indicating its suitability for high-throughput screening applications and drug development.

With the emergence of extensively drug-resistant strains of *Mycobacterium tuberculosis* (*M. tb*)[1] [1], there is growing interest in the study of drug resistance mechanisms. In addition to identified and characterized molecular mechanisms, *M. tb* antibiotic resistance is aided by the very low permeability of its thick hydrophobic cell envelope [2]. The cell wall of *M. tb* is characteristic of the genus and is made of four major components: the plasma membrane (PM), the peptidoglycan (PG), the arabinogalactan (AG) matrix containing a covalently linked complex of mycolic acids, and the outer capsule-like layer. The PG, anchored in the PM, is covalently linked to the AG through a diglycosyl phosphoryl bridge. The resulting arabinogalactan–peptidoglycan complex (AGP) is esterified at the nonreducing ends, with mycolic acids forming a mycolyl–arabinogalactan–peptidoglycan complex (mAGP). A layer of free glycolipids interacts with the mycolyl moiety of the mAGP. Finally, the outermost layer is a mixture of polysaccharides and proteins called the capsule.

Enzymes involved in the maintenance of the bacterial cell wall are of extreme importance to mycobacteria. The relative success of antitubercular drugs such as isoniazid (INH), ethambutol (EMB), ethionamide (ETH), and thiacetazone (TAC) targeting the biosynthesis of cell wall components illustrates this [3]. Another class of enzymes known to be involved in the maintenance of the mycobacterial cell wall is the antigen 85 complex (Ag85). This family of proteins was first isolated as the major secreted component of *M. tb* culture filtrates [4]. Three homologous proteins compose Ag85: antigen 85A (Ag85A), antigen 85B (Ag85B), and antigen 85C (Ag85C). The proteins bear a high amino acid sequence identity (68–79%) in their mature secreted forms, but surprisingly the genes encoding Ag85 are in separate loci of the *M. tb* genome [5]. In addition to being the immunodominant antigens, the proteins were characterized as mycolyltransferases using a radiometric assay [6]. This assay indicated that the enzymes are involved in the formation of the glycolipid trehalose dimycolate (TDM), also called cord factor.

Further studies *in vivo*, relying on the disruption of Ag85 genes, resulted in a variety of observations. The inactivation of the *fbpC2* (fibronectin binding protein C2) gene that encodes Ag85C resulted in 40% less cell wall bound mycolates but produced no change in

* Corresponding author. Fax: +1 419 530 4033.
E-mail address: donald.ronning@utoledo.edu (D.R. Ronning).

[1] *Abbreviations used: M. tb, Mycobacterium tuberculosis;* PM, plasma membrane; PG, peptidoglycan; AG, arabinogalactan; AGP, arabinogalactan–peptidoglycan complex; mAGP, mycolyl–arabinogalactan–peptidoglycan complex; INH, isoniazid; EMB, ethambutol; ETH, ethionamide; TAC, thiacetazone; Ag85, antigen 85 complex; Ag85A, antigen 85A; Ag85B, antigen 85B; Ag85C, antigen 85C; TDM, trehalose dimycolate; TMM, trehalose monomycolate; HTS, high-throughput screening; $CHCl_3$, chloroform; EtOAc, ethyl acetate; CH_2Cl_2, methylene chloride; MeOH, methanol; DMSO, dimethyl sulfoxide; DMAP, dimethylaminopyridine; DIPEA, diisopropylethylamine; NaH, sodium hydride; TLC, thin-layer chromatography; ESI–MS, electrospray ionization–mass spectrometry; LC, liquid chromatography; HRMS, high-resolution mass spectrometry; SDS–PAGE, sodium dodecyl sulfate–polyacrylamide gel electrophoresis; AChEs, acetylcholinesterase; PKS–TE, polyketide synthase thioesterase.

0003-2697/$ - see front matter © 2008 Elsevier Inc. All rights reserved.
doi:10.1016/j.ab.2008.10.018

the quantity of noncovalently bound lipids such as TDM [7]. The decrease in bound mycolates seen in the 85C knockout greatly increased the permeability of the cell wall for hydrophobic and small hydrophilic compounds [7]. However, the ability of INH to permeate the cell envelope was not affected. Inactivation of the genes encoding 85A and 85B had no apparent effect on the levels of TDM or covalently linked mycolates [7,8]. In addition, growth of cultured mycobacteria was also not affected. Overall, these studies demonstrate that the *in vitro* mycolyltransferase activity is also observed *in vivo* and that, because Ag85A and Ag85B could not compensate for the inactivation of *fbpC2*, the three enzymes of Ag85 are not fully redundant.

In a separate study, the disruption of *fbpA*, the gene encoding Ag85A, resulted in poor growth in a macrophage-like cell line, ultimately leading to the death of the mycobacteria. In contrast, disruption of *fbpB*, the gene encoding Ag85B, did not have any effect on mycobacterial survival [8]. Another study showed significant inhibition of *M. tb* growth in culture when the three *fbp* transcripts were targeted by modified oligodeoxyribonucleotides to inhibit translation [9,10]. Even though no clear evidence of a bactericidal effect of Ag85 inactivation was reported, the authors did show that the effect was bacteriostatic, representing a significant achievement. Combination of this antisense technology with INH produced a synergistic bactericidal effect, indicating that a drug targeting Ag85 could greatly improve combination therapy for tuberculosis [10]. Moreover, a successful drug targeting all three enzymes from the complex decreases the likelihood of resistance because the odds that mutations occur in all three targets at the same time in the same organism are infinitesimal.

Another rationale for targeting Ag85 is its extracellular localization. The typical bacterial artillery against antibiotics, such as efflux pumps within the bacterial membrane and drug-modifying enzymes acting intracellularly, would have little effect on drugs targeting Ag85 [11,12]. Finally, because the mycolyltransferases are not found in humans, the xenobiotic nature of any specific inhibitor containing trehalose or arabinose moieties targeting those enzymes would present minimal side effects.

The discovery of lead compounds that inhibit Ag85 necessitates a rapid and easy assessment of the activity of the enzymes in the presence of inhibitors. The only previously published mycolyltransferase assay involves the isolation of trehalose monomycolate (TMM) from *M. tb* and the enzymatic transfer of mycolic acids from a lipid-soluble TMM molecule to a radioactive water-soluble trehalose molecule and the manipulation of the radioactive products in a two-phase reaction. A subsequent aqueous workup with extraction and thin layer chromatography allows visualization of the products [6]. Although the radiometric assay works well, it requires the use of radioactive-labeled molecules and is relatively slow. High-throughput screening (HTS) of large numbers of potential inhibitors is not feasible using this assay; therefore, a faster assay is needed. For development of a proof-of-concept HTS assay, a spectrophotometric method seemed to be the best candidate.

When developing this assay, two major criteria needed to be met. First, the synthetic substrate must be of sufficient similarity to the natural substrate to ensure specificity to the primary enzyme. Second, the reaction velocity must represent the enzymatic activity of the primary enzyme and not that of any linked enzymes. These two criteria ensure that data obtained from the assay are biologically relevant, and this is especially important when using the assay for inhibitor screening. Because this assay was conceived specifically for use in identifying lead compounds that inhibit Ag85, labeling the substrate with a chromogenic moiety offered the most robust assay with the highest potential sensitivity [13].

Structural and mechanistic considerations guided the design of the acyl donor. Because Ag85 catalyzes the transfer of mycolate from trehalose to other carbohydrates [6,8], the assay requires a carbohydrate-based substrate that functions as the acyl donor in the same way as TMM functions as the mycolyl donor *in vivo*. Because TMM is highly insoluble in water, shortening the fatty acyl chain was essential to improve substrate solubility. Based on the crystal structure of Ag85A bound to octylthioglucoside, an octanoyl chain seemed to be a reasonable compromise between solubility and mycolic acid mimicry to ensure enzyme binding [14]. Because the mycolic acid in TMM is linked at the O6 position of the glucose moieties in trehalose, an octanoyl moiety linked at O6 of glucose is a reasonable structural analog. Therefore, a glucose derivative with an acyl chain should bear enough structural similarities with the natural substrate to be recognized by the enzyme. In addition, the active site of the Ag85 enzymes readily accommodates a variety of carbohydrates and glycoconjugates. Both disaccharide molecules such as trehalose [15,16] and glycoconjugates containing alkyl moieties such as octylthioglucoside [14] have been shown to bind within the active sites of Ag85B and Ag85C. Both structures indicate that ample space is available for a glucoside modified with a moderately sized chromophore. In the carbohydrate chemistry and chemical biology fields, glycosidases and *p*-nitrophenyl-containing compounds are used extensively, resulting in many examples of O1 modification of glucose with *p*-nitrophenyl, or another of a large variety of chromophores and fluorophores, that can be readily cleaved by glucosidases [17,18]. Based on these previous studies, a glucose derivative esterified at the sixth position with an eight-carbon acyl chain and a *p*-nitrophenyl moiety attached by a β-linkage onto O1 of glucose was chosen as the substrate for the assay.

The coupled assay proceeds in two steps (Fig. 1). A nucleophilic attack on the ester linkage of the octanoyl chain by Ag85C releases *p*-nitrophenyl-β-D-glucoside, which is then hydrolyzed by β-glucosidase into glucose and *p*-nitrophenolate. The rate of *p*-nitrophenolate release is observed by direct measurement of the absorbance over time. An excess of D-glucose is added to the reaction to function as an acyl acceptor and to promote turnover of the enzyme. This article describes the development of this spectrophotometric

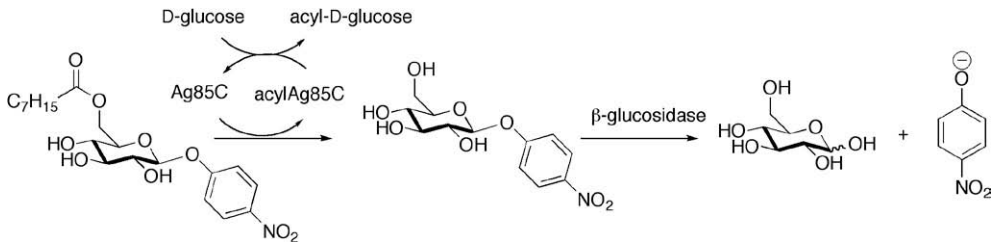

Fig. 1. Coupled colorimetric acyl-transfer assay. The serine nucleophile from Ag85 attacks the ester linkage and releases the *p*-nitrophenyl-β-D-glucoside. β-Glucosidase then hydrolyzes the glycosidic bond of the glucoside, producing D-glucose and *p*-nitrophenolate. Measuring the absorbance at 405 nm allows direct monitoring of the change in *p*-nitrophenolate concentration. The Ag85C acyl-enzyme intermediate reacts with D-glucose to regenerate the apo form of Ag85C.

Please cite this article in press as: J. Boucau et al., A coupled assay measuring *Mycobacterium tuberculosis* antigen 85C enzymatic ..., Anal. Biochem. (2008), doi:10.1016/j.ab.2008.10.018

acyltransferase assay for Ag85C, initial characterization of enzymatic parameters, and the validation of the assay for HTS applications.

Materials and methods

Materials

D-Glucose, acetone, chloroform ($CHCl_3$), ethyl acetate (EtOAc), hexanes, methylene chloride (CH_2Cl_2), methanol (MeOH), dimethyl sulfoxide (DMSO), pyridine, and toluene were purchased from Fisher; *p*-nitrophenyl-β-D-glucopyranoside and thiazolidine-2-thione were purchased from Sigma–Aldrich; and dimethylaminopyridine (DMAP), diisopropylethylamine (DIPEA), sodium hydride (NaH), and octanoyl chloride were purchased from Acros and were used without purification. All solvents were used as received except pyridine and CH_2Cl_2, which were dried and distilled following standard procedures [19]. Silica (230–400 mesh) for column chromatography was obtained from Sorbent Technologies, and thin-layer chromatography (TLC) precoated plates were obtained from EMD. TLCs (silica gel 60, f_{254}) were visualized under UV light or by charring (5% H_2SO_4–MeOH). Flash column chromatography was performed on silica gel (230–400 mesh) using solvents as received. ^{1}H NMR were recorded on either a Varian VXRS 400 MHz spectrometer or a Varian INOVA 600-MHz spectrometer in $CDCl_3$ or DMSO-D_6 using residual $CHCl_3$ or DMSO as internal reference, respectively. ^{13}C NMR were recorded on a Varian INOVA 150.83 MHz spectrophotometer in $CDCl_3$ using the triplet centered at δ77.23 as internal reference. Mass spectra (electrospray ionization–mass spectrometry [ESI–MS]) were recorded on a Bruker Daltonics Esquire liquid chromatography LC-MS mass spectrometer. High-resolution mass spectrometry (HRMS) was performed on a Micromass Q-TOF2 instrument.

Synthesis of p-nitrophenyl 6-O-octanoyl-β-D-glucopyranoside

The alkylating agent was prepared by treating thiazolidine-2-thione with octanoyl chloride in the presence of DIPEA in anhydrous CH_2Cl_2 in 88% yield (see Fig. 2 and supplementary Material). Esterification of *p*-nitrophenyl-β-D-glucopyranoside with the activated *N*-octanoylthiazilidine-2-thione alkylating agent gives the desired *p*-nitrophenyl 6-*O*-octanoyl-β-D-glucopyranoside in 44% yield (see Fig. 2 and supplementary Material) [20,21].

Molecular cloning

The portion of the *M. tb fbpC2* gene encoding the secreted form of Ag85C lacking a stop codon was amplified by polymerase chain reaction and placed in pET-29 (EMD Biosciences) using *Nde*I and *Xho*I restriction enzymes (New England Biolabs). The resulting open reading frame produces a protein with a C-terminal 6× histidine tag.

Protein purification of Ag85C

The expression plasmid pET29–Ag85C was transformed into T7 express cells (New England Biolabs). The bacterial cells were cultured at 37 °C in Terrific Broth (Research Products International) to an optical density of 1.2 at 600 nm. The culture was then cooled to 16 °C for 1 h, and protein expression was induced with the addition of isopropyl β-D-1-thiogalactopyranoside (Anatrace) at 1 mM. The bacterial cells were harvested by centrifugation after 16 h of incubation at 16 °C. The pelleted cells were resuspended in binding buffer (20 mM sodium phosphate [pH 7.5] and 5 mM β-mercaptoethanol) and were stored at −80 °C until used for protein purification.

The frozen aliquot of resuspended cells was thawed at room temperature and then placed on ice. Then 1 mM of lysozyme (Sigma–Aldrich) and 0.1 mM of DNase1 (Sigma–Aldrich) were added to the suspension for catalytic hydrolysis of undesired components. The catalysis step was performed for 20 min on ice prior to lysis of the cells by sonication (Sonicator 3000, Misonix). The obtained suspension was clarified by high-speed centrifugation (11,000 rpm, fixed-angle rotor, 5810-R Centrifuge, Eppendorf). The pellet component was discarded, and the supernatant was filtered through an immobilized 0.22-μm membrane (Millex-GP, Millipore). The protein was first purified by immobilized metal affinity chromatography. A HisTrap FF 5 mL column (GE Healthcare) was used on a fast protein liquid chromatography system (ÄktaFPLC, Amersham Biosciences). The fractions containing Ag85C were pooled and diluted fivefold into binding buffer and subsequently were run on an ion exchange chromatography column (HiTrap Q FF, GE Healthcare) on the ÄktaFPLC system. The fractions containing Ag85C were pooled, and solid ammonium sulfate was added to a concentration of 2.4 M. The precipitated protein was pelleted by centrifugation and resuspended in crystallization buffer (10 mM Tris [pH 7.5], 2 mM ethylenediaminetetraacetic acid, and 1 mM dithiothreitol). The final purification step used size exclusion chromatography on a Superdex 200 prep-grade column (XK 16/60, Amersham Biosciences) equilibrated with crystallization buffer (Fig. 3). The fractions containing Ag85C were pooled and stored at −80 °C until needed for the assay.

Enzyme concentration determination

The enzyme concentration was determined using absorbance spectroscopy with 280 nm wavelength light. The extinction coef-

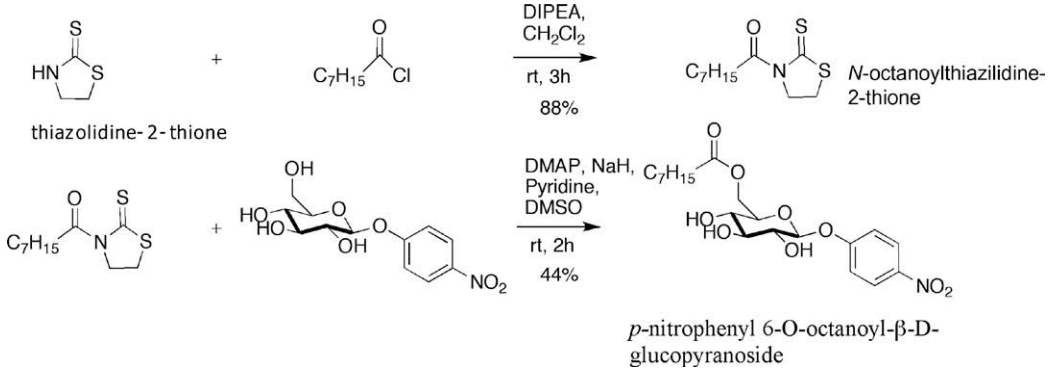

Fig. 2. Synthetic scheme of the Ag85C acyl donor substrate. Reactants for the two synthetic steps are shown. All products were analyzed by ^{1}H NMR, ^{13}C NMR, and LC–MS (see supplementary material). The *p*-nitrophenyl 6-*O*-octanoyl-β-D-glucoside represents the acyl-donor substrate used in this study.

Please cite this article in press as: J. Boucau et al., A coupled assay measuring *Mycobacterium tuberculosis* antigen 85C enzymatic ..., Anal. Biochem. (2008), doi:10.1016/j.ab.2008.10.018

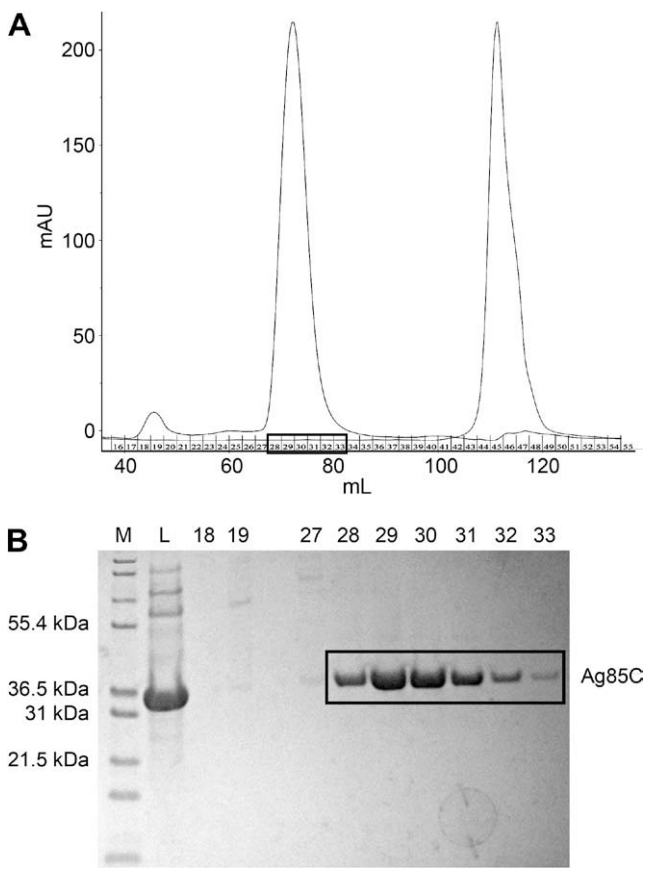

Fig. 3. Size exclusion chromatogram and corresponding SDS–PAGE results. (A) The fractions containing purified enzyme are surrounded by the black box. Fractions representing the Ag85C peak, the fractions at the void volume of the column, and the loaded sample were subjected to SDS–PAGE. Both A_{280nm} and conductivity traces are shown. (B) A Coomassie-stained SDS–PAGE gel shows the sample loaded onto the Superdex 200 column and the protein components of the eluted fractions. M, marker; L, sample injected onto column; numbers represent the corresponding eluted fractions. From the gel, it is clear that fractions 28 to 33 contain significant amounts of highly purified Ag85C.

ficient was obtained from computational calculations on the ExPASy website [22]. The predicted extinction coefficient for the recombinant Ag85C protein was 84,340 $M^{-1}cm^{-1}$. An additional absorbance reading at 260 nm allowed the calculation of the A_{280nm}/A_{260nm} ratio to confirm that the A_{280nm} value represents the true protein concentration and not the concentration of a protein/nucleic acid mixture. The typical A_{280nm}/A_{260nm} ratio for purified Ag85C used in the assay was 1.97, indicating that little or no nucleic acid was present in the sample. The experiments were performed on a Genesys 6 spectrophotometer (Thermo Electron) with a 1 cm pathlength.

Control experiments and standard curves

A 0.2 mM solution of *p*-nitrophenol was prepared using the buffer conditions of the assay (50 mM sodium phosphate [pH 7.4], 3 mM D-glucose, and 2% DMSO). A wavelength scan experiment (340–800 nm) was then performed on the absorbance plate reader (SpectraMax 340PC, Molecular Devices). The data were exported from Molecular Devices SoftMax Pro5 software and analyzed in GraphPad Prism 5 software.

The extinction coefficient of *p*-nitrophenolate in the reaction buffer was determined from calibration curve studies with standard *p*-nitrophenol solutions. A range of solutions (0.5–300 μM) was prepared by serial dilution of a stock 0.1 M *p*-nitrophenol solution. The absorbance of each solution at 405 nm was measured on the plate reader. The data from three independent experiments were exported from SoftMax Pro5 and analyzed in GraphPad Prism 5 to yield the standard curve.

The negative and positive control experiments and the Ag85C concentration course experiments were run following the assay procedure described hereafter. For the control experiments, the relevant enzymes were omitted. For the concentration course, various amounts of Ag85C enzyme (0.01–1.5 μM) were used with other components held constant.

Standard acyltransferase assay

The assay was performed under atmospheric pressure at room temperature in a 96-well plate format. The synthetic substrate was dissolved and stored in 100% DMSO. In each assay reaction, the following components and an appropriate volume of buffer were combined, resulting in a total reaction volume of 100 μL. A master mix was prepared with 2 units of β-glucosidase (Sigma–Aldrich), 3 mM of D-glucose (Fisher Scientific), 50 mM sodium phosphate (pH 7.4), and 1% DMSO. The 1 μL of the substrate in DMSO solution was added to each well to reach the desired substrate concentration (10–200 μM) followed by the addition of Ag85C to a final concentration of 100 nM. The release of the signaling molecule, *p*-nitrophenolate, was monitored by measurement of the absorbance at 405 nm every 30 s for 1 h.

β-Glucosidase concentration course

The glucosidase concentration course was performed under the same conditions as mentioned above except that the final Ag85C concentration was increased to 200 nM to improve the signal for the reactions at low β-glucosidase concentrations. The β-glucosidase concentrations were varied from 0.1 to 5 units/reaction.

Data analysis

The data were exported from Molecular Devices SoftMax Pro5 software, and initial velocity (V_i) values were calculated using Microsoft Excel. The data were normalized using negative controls (no Ag85C added). The V_i values were entered into GraphPad Prism 5 to determine K_m and V_{max} values. Z' values from the positive and negative controls were calculated using the V_i values to validate the assay for inhibitor screening [23].

Results and discussion

Purification of Ag85C

The published purification protocol for Ag85C is sufficient for crystallization studies [14,15]. However, to eliminate contaminating nucleic acids and obtain an A_{280nm} reading that represents the Ag85C protein concentration most accurately, an additional column chromatography step was required. Subjecting Ag85C to anion exchange chromatography removes the contaminating nucleic acids as measured by UV–visible absorption spectroscopy at wavelengths of both 280 and 260 nm. The final purification step involves size exclusion chromatography (Fig. 3A) and results in highly purified Ag85C as exhibited by sodium dodecyl sulfate–polyacrylamide gel electrophoresis (SDS–PAGE) (Fig. 3 B).

Determination of assay parameters

To determine the optimal wavelength to monitor the release of *p*-nitrophenolate during the assay, a wavelength scan was performed with a stock *p*-nitrophenol solution (Fig. 4A).

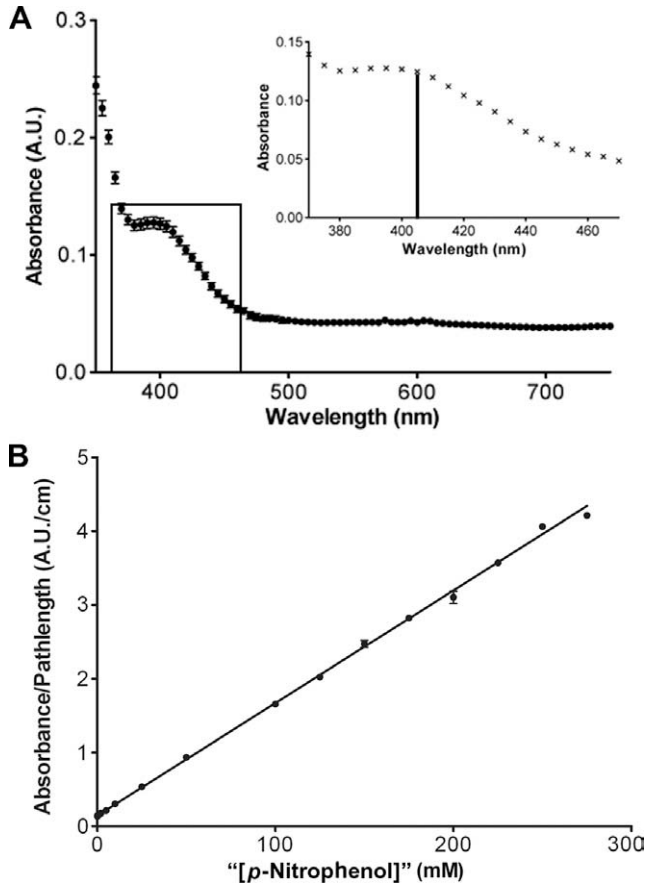

Fig. 4. Characterization of *p*-nitrophenol in assay conditions. (A) Wavelength scan of *p*-nitrophenol in reaction buffer. Purchased *p*-nitrophenol was added to the assay reaction buffer to determine the absorption maximum of the compound under conditions of the acyl-transfer assay. Although the absorption peak is near 395 nm, 405 nm was chosen for consistency with previously published data. (B) Standard curve for *p*-nitrophenol. A concentration course of *p*-nitrophenol versus absorbance at 405 nm in standard buffer conditions is shown. These data were used to determine the extinction coefficient for the *p*-nitrophenolate product in the assay.

The curve reaches an absorption maximum at 395 nm. However, to be consistent with current literature, an absorbance of 405 nm was chosen for the assay. Because the value of the molar extinction coefficient varies depending on the assay conditions and the wavelength, absorbance readings of *p*-nitrophenol solutions at various concentrations were carried out in the assay conditions. The plotted values of absorbance over pathlength versus *p*-nitrophenol concentration yielded a linear plot with a correlation coefficient (r^2) of 0.99. The extinction coefficient was calculated from these data to be 15,300 $M^{-1} cm^{-1}$ (Fig. 4B).

Control reactions were carried out in the presence and absence of both enzymes to ensure that the assay was functioning as expected and that each step of the assay was dependent on the presence of all components (Fig. 5). Without any enzyme present, there is no increase in absorbance observed over time, meaning that the chromophore is not released by nonenzymatic hydrolysis under current assay conditions. The addition of β-glucosidase caused a slight increase in absorbance over time, indicating that β-glucosidase displays a low activity against the synthetic substrate resulting in a slow release of the chromophore. The addition of Ag85C to the mixture produced a significant increase of absorbance over time that results from the deacylation of the starting substrate followed by a relatively rapid release of the chromophore catalyzed by β-glucosidase. The background reaction due to hydrolysis of the acylated synthetic substrate by β-glucosidase was measured, and the initial velocity values were subtracted from assay values for rigorous analysis of the data.

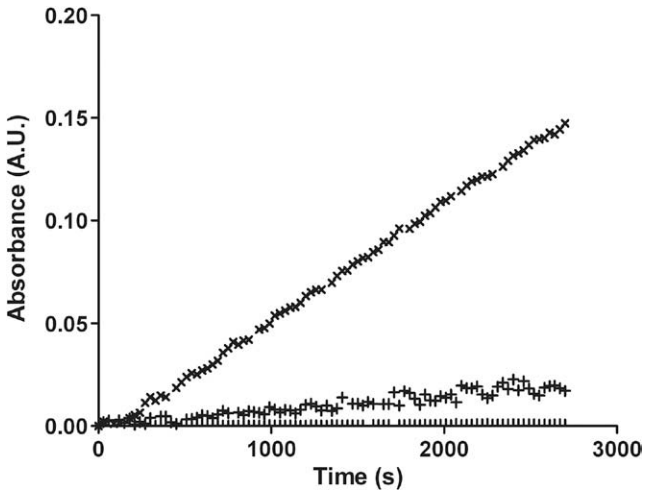

Fig. 5. Positive and negative control reactions. Reactions were performed with no enzyme (|), glucosidase only (+), Ag85C, and glucosidase (×). The concentration of the substrate in each reaction was 175 μM.

Once the preliminary parameters were fixed, an Ag85C concentration course experiment determined the optimal concentration

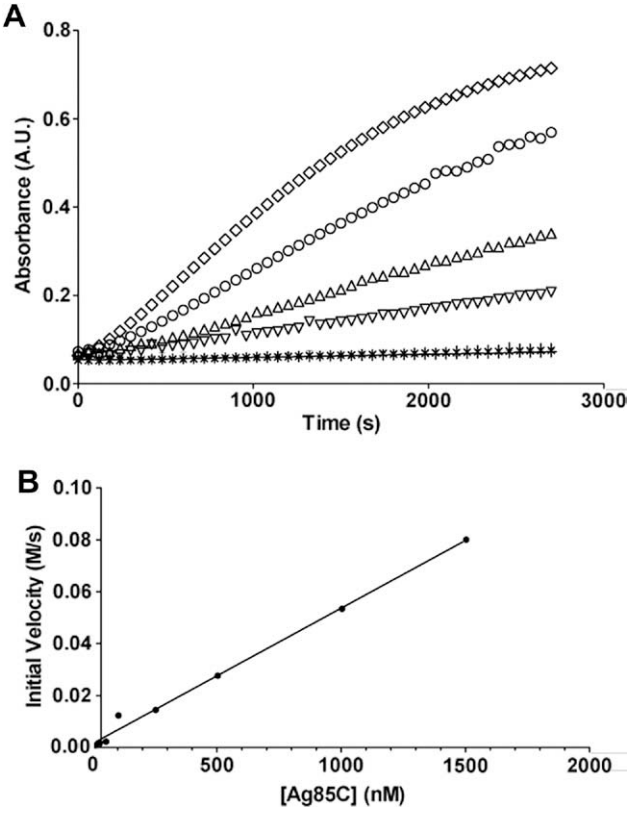

Fig. 6. Relationship between enzyme concentration and catalytic rate exhibited by the assay. (A) Raw data from the assay illustrate the increasing rate of *p*-nitrophenolate production as Ag85C is increased. Concentrations of Ag85C tested are 10 nM (–), 25 nM (+), 50 nM (×), 100 nM (|), 250 nM (▽), 500 nM (Δ), 1000 nM (○), and 1500 nM (◇). The data for the four lowest enzyme concentrations are superimposed in this plot. Linear regression allowed initial velocity values to be determined. (B) Initial velocity values as a function of Ag85C concentration. The initial velocity values obtained from assays performed with varying enzyme concentrations show a linear relationship between velocity and Ag85C concentration.

Please cite this article in press as: J. Boucau et al., A coupled assay measuring *Mycobacterium tuberculosis* antigen 85C enzymatic ..., Anal. Biochem. (2008), doi:10.1016/j.ab.2008.10.018

of Ag85C (Fig. 6). The initial velocity values were calculated for each Ag85C concentration and were plotted (Fig. 6B). The plot shows a linear correlation between the initial velocity values and the concentration of Ag85C with a correlation factor of 0.99. This experiment determined the range of Ag85C concentrations that lead to a linear change in the rate of the reaction and that, under the current assay conditions, Ag85C appears to catalyze the slowest step of the coupled assay.

To ensure that β-glucosidase is not limiting, a similar concentration course approach was used where β-glucosidase concentrations were varied. Reactions were performed in the standard conditions with the following exceptions. Twice the Ag85C concentration of the standard assay was used (200 nM), and the substrate concentration was fixed at 175 μM. The data shown in Fig. 7 illustrate that the V_i for each reaction increases with respect to β-glucosidase concentration between 0.1 and 1 unit/reaction. At β-glucosidase concentrations of 1 unit/reaction and higher, the initial velocity peaks near 0.02 μM/s, indicating that the Ag85C activity is now limiting the velocity of the reaction. Based on these data, a concentration of 2 units/reaction, or 20 units/mL, of β-glucosidase was used for all subsequent assays.

With all of the above experiments in mind, ultimately the following assay parameters were chosen because they led to consistent results while using a minimal amount of reagents: 100 nM Ag85C, 2 units of β-glucosidase, 3 mM D-glucose, and 2% DMSO.

Assay validation

The Z' factor, a statistical parameter, was developed for the evaluation of the inherent signal-to-noise ratio and to quantitatively represent assay reproducibility [23]. To determine this parameter for the described assay, the V_i values for a series of negative and positive controls were measured. For the negative control assay, reactions were performed in the presence of β-glucosidase but lacking Ag85C. The positive control reactions were performed using assay conditions mentioned previously. Two separate sets of 16 control experiments were used to evaluate Z'. From these data, the calculated Z' value was determined to be 0.81 ± 0.06, thereby indicating an excellent signal-to-noise ratio for the assay and that it is suitable for HTS applications.

Enzyme kinetics

Once assay parameters were defined, we performed a series of experiments under conditions of varying substrate concentrations to determine the kinetic parameters of the acyl-transfer reaction catalyzed by Ag85C. The absorbance versus time graphs provided the data to determine the initial velocity values of each reaction. Plotting V_i versus substrate concentrations produced curves resembling those expected for enzymes obeying Michaelis–Menten kinetics. The data were fit to the Michaelis–Menten model (Fig. 8) to determine the kinetic parameters V_{max} and K_m, which were calculated to be 0.0062 ± 0.0003 μM/s and 0.047 ± 0.008 mM, respectively ($r^2 = 0.92$). This V_{max} value corresponds to a reasonable k_{cat} value of 0.062 s^{-1}.

The K_m value determined for the Ag85C assay using the synthetic substrate is similar to that seen for other members of the α/β hydrolase superfamily of enzymes, the fold family to which Ag85 belongs. Other well-characterized members of this fold family include acetylcholinesterase (AChEs) and polyketide synthase thioesterase (PKS–TE). Kinetic studies with AChEs from the electric eel and PKS–TE from *Bacillus brevis* have shown these enzymes to possess K_m values of 100 and 3 μM, respectively [24,25]. These K_m values are quite similar to the value observed in our assay, indicating that the synthetic Ag85 substrate performs well in mimicking the natural substrate.

In contrast, the k_{cat} value for Ag85C is much lower than that observed for other α/β hydrolases such as AChEs [24] and other carboxylesterases [26]. These enzymes have very high turnover numbers on the orders of 10^4 or 10^5 s^{-1}. However, the k_{cat} for Ag85C is more reflective of the value measured for the PKS–TE [25]. The reasons for these differences are not clear, but one can rationalize that the k_{cat} values may reflect the identity of the nucleophile in the second step of the enzymatic reaction. AChEs and carboxylesterases use water as the nucleophile to disrupt the acyl-enzyme intermediate, whereas Ag85 and PKS–TE do not. Rather, PKS–TE relies on an intramolecular nucleophilic attack at the thioester linkage that produces the cyclic product and allows release from the active site. The relatively low turnover number of 1 s^{-1} possibly reflects the requirement of a structural change in the substrate to promote this attack. The Ag85 mechanism goes a step further and requires an intermolecular nucleophilic attack, which further depresses the turnover rate with respect to PKS–TE. However, although the described assay uses D-glucose as the acyl acceptor at a 3 mM concentration, this might not reflect the concentration encountered by the enzyme *in vivo*. Further experiments using liposomes or micelles harboring the substrate may give a more biologically relevant representation of the k_{cat} value for Ag85C.

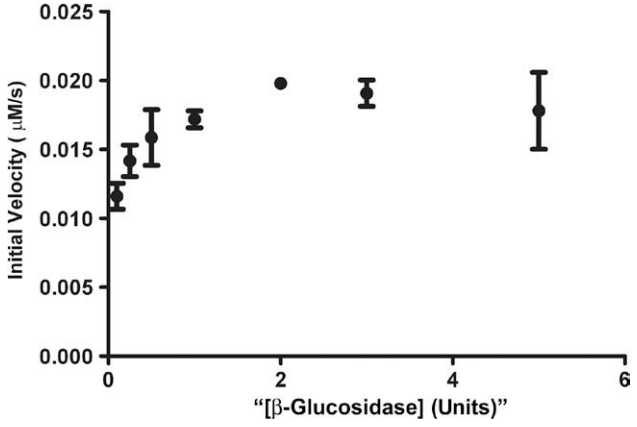

Fig. 7. Reaction velocity is limited by the activity of Ag85C. This plot shows initial velocity from reactions performed with varying concentrations of β-glucosidase. Ag85C was fixed at 200 nM, and the synthetic substrate was kept at a constant concentration of 175 μM. These data show that no increase in reaction velocity is observed at β-glucosidase concentrations higher than 1 unit/reaction.

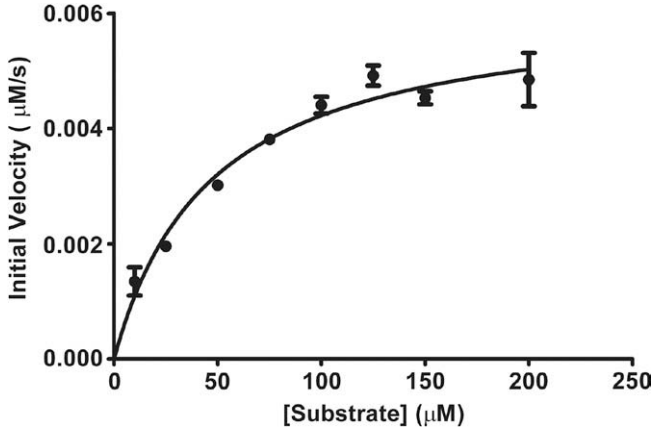

Fig. 8. Determination of Ag85C kinetic parameters. Assays were performed 12 times for each substrate concentration, and data from the first 500 s from each reaction were subjected to linear regression analysis to obtain initial velocities. Those V_i values are plotted against substrate concentration. The K_m and V_{max} values were obtained by fitting these data to the Michaelis–Menten equation.

Please cite this article in press as: J. Boucau et al., A coupled assay measuring *Mycobacterium tuberculosis* antigen 85C enzymatic ..., Anal. Biochem. (2008), doi:10.1016/j.ab.2008.10.018

Another possibility for the relatively low Ag85C k_{cat} value is the required conformational change that occurs during catalysis. The crystal structure of Ag85C covalently modified at S124 clearly indicates a conformational change in the enzyme as a direct consequence of forming the acyl-enzyme intermediate [15]. The consequences of this conformational change are twofold. First, residue H260, the general base in the first step of the catalytic reaction, has moved away from the active site nucleophile, S124. This precludes H260 from acting as the general base in the second enzymatic step. Second, the region encompassing residues 210 to 221 has changed significantly in conformation, resulting in the repositioning of this loop near the active site leading to modification of the carbohydrate binding pocket. This would seem to preclude Ag85C from using trehalose as an acyl acceptor [15,16], but available enzymatic data clearly show acyl transfer to trehalose [6].

These two structural consequences seem to expand the substrate binding and catalytic repertoire of Ag85C. However, requiring the repositioning of a general base to activate a hydroxyl moiety on the acyl acceptor to promote nucleophilic attack on the acyl-enzyme intermediate may have also led to the significantly lower Ag85C k_{cat} value in relation to that of PKS–TE.

Conclusion

This article has presented the development of a colorimetric assay for the measurement of Ag85C enzymatic activity. Initial results from this assay show a reproducible rate response to changes in either substrate concentration or Ag85C concentration. We have also shown that, under the current reaction regime, Ag85C concentration determines the initial velocity in the assay, allowing accurate determination of kinetic parameters defined for Ag85C by Michaelis–Menten kinetics.

The kinetic parameters obtained for Ag85C for the synthetic substrate indicate that there is room for improvement in both substrate specificity and solubility. In addition, the large size of the carbohydrate binding pocket in the Ag85C active site makes this system a prime candidate for improvement by using a fluorogenic moiety on the synthetic substrate to improve the sensitivity of the assay. However, the calculated Z' value of 0.81 indicates that the assay already exhibits an excellent signal-to-noise ratio and so improvement is not essential for library screening.

The design of the assay focused on requiring a very small reaction volume, making it immediately amenable to HTS applications. We completed the screening of a small drug library as proof-of-principle for the coupled assay. A hit rate of 3% was obtained, with the best inhibitory compounds showing a 90% decrease in the reaction velocity. This inhibitory activity is reciprocated in a Kirby–Bauer disk assay using *Mycobacterium smegmatis* as a surrogate for *M. tuberculosis.* Observable zones of inhibition again validated Ag85C as a good drug target by confirming that growth inhibition of mycobacteria can be affected by inhibiting Ag85C activity. Use of the described assay will certainly aid in both lead identification and structure–activity relationship studies for new Ag85 inhibitors and antitubercular drugs.

As further evidence of the versatility of this assay, we recently described characterization of mono- and diacylated arabinofuranosides that are produced when reacting Ag85C with the acyl donor and using, as the acyl acceptor, a diarabinofuranoside that mimics the nonreducing termini of the mycobacterial AG [27]. Current work is, and future work will be, focused on better understanding of the substrate specificity and substrate range of all three enzymes of the Ag85 complex.

Acknowledgments

We thank the deArce Memorial Endowment Fund in Support of Medical Research and Development for its generous support. We also thank the Department of Chemistry at the University of Toledo for its support and the University Research Awards and Fellowship program for an Interdisciplinary Research Initiation Award that helped to support this research.

Appendix A. Supplementary data

Supplementary data associated with this article can be found, in the online version, at doi:10.1016/j.ab.2008.10.018.

References

[1] N.R. Gandhi, A. Moll, A.W. Sturm, R. Pawinski, T. Govender, U. Lalloo, K. Zeller, J. Andrews, G. Friedland, Extensively drug-resistant tuberculosis as a cause of death in patients co-infected with tuberculosis and HIV in a rural area of South Africa, Lancet 368 (2006) 1575–1580.
[2] P. Draper, M. Daffe, The cell envelope of *Mycobacterium tuberculosis* with special reference to the capsule and outer membrane permeability barrier, in: S.T. Cole K.D. Eisenach D.N. McMurray (Eds.), Tuberculosis and the Tubercle Bacillus, ASM Press, Washington, DC, 2005, pp. 261–273.
[3] Y. Zhang, C. Vilcheze, W.R. Jacobs, Mechanisms of drug resistance in *Mycobacterium tuberculosis*, in: S.T. Cole K.D. Eisenach D.N. McMurray (Eds.), Tuberculosis and the Tubercle Bacillus, ASM Press, Washington, DC, 2005, pp. 115–140.
[4] M. Yoneda, Y. Fukui, Isolation, purification, and characterization of extracellular antigens of *Mycobacterium tuberculosis*, Am. Rev. Respir. Med. 92 (1965) 9–18.
[5] G. Harth, B.Y. Lee, J. Wang, D.L. Clemens, M.A. Horwitz, Novel insights into the genetics, biochemistry, and immunocytochemistry of the 30-kilodalton major extracellular protein of *Mycobacterium tuberculosis,*, Infect. Immun. 64 (1996) 3038–3047 (Erratum appears in Infect. Immun. (1997) 852).
[6] J.T. Belisle, V.D. Vissa, T. Sievert, K. Takayama, P.J. Brennan, G.S. Besra, Role of the major antigen of *Mycobacterium tuberculosis* in cell wall biogenesis, Science 276 (1997) 1420–1422.
[7] M. Jackson, C. Raynaud, M.A. Laneelle, C. Guilhot, C. Laurent-Winter, D. Ensergueix, B. Gicquel, M. Daffe, Inactivation of the antigen 85C gene profoundly affects the mycolate content and alters the permeability of the *Mycobacterium tuberculosis* cell envelope, Mol. Microbiol. 31 (1999) 1573–1587.
[8] V. Puech, C. Guilhot, E. Perez, M. Tropis, L.Y. Armitige, B. Gicquel, M. Daffe, Evidence for a partial redundancy of the fibronectin-binding proteins for the transfer of mycolyl residues onto the cell wall arabinogalactan termini of *Mycobacterium tuberculosis*, Mol. Microbiol. 44 (2002) 1109–1122.
[9] G. Harth, M.A. Horwitz, D. Tabatadze, P.C. Zamecnik, Targeting the *Mycobacterium tuberculosis* 30/32-kDa mycolyl transferase complex as a therapeutic strategy against tuberculosis: Proof of principle by using antisense technology, Proc. Natl. Acad. Sci. USA 99 (2002) 15614–15619.
[10] G. Harth, P.C. Zamecnik, D. Tabatadze, K. Pierson, M.A. Horwitz, Hairpin extensions enhance the efficacy of mycolyl transferase-specific antisense oligonucleotides targeting *Mycobacterium tuberculosis*, Proc. Natl. Acad. Sci. USA 104 (2007) 7199–7204.
[11] X. Hanoulle, J.M. Wieruszeski, P. Rousselot-Pailley, I. Landrieu, C. Locht, G. Lippens, A.R. Baulard, Selective intracellular accumulation of the major metabolite issued from the activation of the prodrug ethionamide in mycobacteria, J. Antimicrob. Chemother. 58 (2006) 768–772.
[12] A. Alahari, X. Trivelli, Y. Guerardel, L.G. Dover, G.S. Besra, J.C. Sacchettini, R.C. Reynolds, G.D. Coxon, L. Kremer, Thiacetazone, An antitubercular drug that inhibits cyclopropanation of cell wall mycolic acids in mycobacteria, PLoS ONE 2 (2007) e1343.
[13] J.P. Goddard, J.L. Reymond, Recent advances in enzyme assays, Trends Biotechnol. 22 (2004) 363–370.
[14] D.R. Ronning, V. Vissa, G.S. Besra, J.T. Belisle, J.C. Sacchettini, *Mycobacterium tuberculosis* antigen 85A and 85C structures confirm binding orientation and conserved substrate specificity, J. Biol. Chem. 279 (2004) 36771–36777.
[15] D.R. Ronning, T. Klabunde, G.S. Besra, V.D. Vissa, J.T. Belisle, J.C. Sacchettini, Crystal structure of the secreted form of antigen 85C reveals potential targets for mycobacterial drugs and vaccines, Nat. Struct. Biol. 7 (2000) 141–146.
[16] D.H. Anderson, G. Harth, M. Horwitz, D. Eisenberg, An interfacial mechanism and a class of inhibitors inferred from two crystal structures of the *Mycobacterium tuberculosis* 30 kDa major secretory protein (antigen 85B), a mycolyl transferase, J. Mol. Biol. 307 (2001) 671–681.
[17] C. Wu, C. Chang, J. Chen, C. Wong, C. Lin, Rapid diversity-oriented synthesis in microtiter plates for in situ screening: Discovery of potent and selective α-fucosidase inhibitors, Angew. Chem. Intl. Ed. 42 (2003) 4661–4664.
[18] J.T. Weadge, A.J. Clarke, *Neisseria gonorrheae O*-acetylpeptidoglycan esterase, A serine esterase with a Ser-His-Asp catalytic triad, Biochemistry 46 (2007) 4932–4941.

[19] W.L.F. Armarego, C.L.L. Chai, Purification of Organic Chemicals, Purification of Laboratory Chemicals, Butterworth–Heinemann, New York, 2003 pp. 80–388.
[20] D. Plusquellec, K. Baczko, Sugar chemistry without protecting groups: a novel regioselective synthesis of 6-O-acyl-D-glucopyranoses and methyl-6-O-acyl-α-D-glucopyranosides, Tetrahedron Lett. 28 (1987) 3809–3812.
[21] D. Plusquellec, F. Roulleau, F. Bertho, M. Lefeuvre, E. Brown, Chemistry of sugars without protective groups: I. Regioselective esterification of the anomeric hydroxyl of lactose, maltose, and glucose, Tetrahedron 42 (1986) 2457–2467.
[22] E. Gasteiger, C. Hoogland, A. Gattiker, S. Duvaud, M.R. Wilkins, R.D. Appel, A. Bairoch, Protein identification and analysis tools on the ExPASy server, in: J.M. Walker (Ed.), The Proteomics Protocols Handbook, Humana Press, Totowa, NJ, 2005, pp. 571–607.
[23] J-H. Zhang, T.D.Y. Chung, K.R. Oldenburg, A simple statistical parameter for use in evaluation and validation of high throughput screening assays, J. Biomol. Screen. 4 (1999) 67–73.
[24] T.L. Rosenberry, S.A. Bernhard, Catalysis by acetylcholinesterase: I. Fluorescent titration with a carbamoylating agent, Biochemistry 10 (1971) 4114–4120.
[25] J.W. Trauger, R.M. Kohli, H.D. Mootz, M.A. Marahiel, C.T. Walsh, Peptide cyclization catalysed by the thioesterase domain of tyrocidine synthetase, Nature 407 (2000) 215–218.
[26] Y.J. Park, S.Y. Choi, H.B. Lee, A carboxylesterase from the thermoacidophilic archaeon *Sulfolobus solfataricus* P1: Purification, characterization, and expression, Biochim. Biophys. Acta 1760 (2006) 820–828.
[27] A.K. Sanki, J. Boucau, D.R. Ronning, S.J. Sucheck, Antigen 85C-mediated acyltransfer between synthetic acyl donors and fragments of the arabinan, Glycoconj. J. (in press), doi:10.1007/s10719-008-9211-z.